FINAL TECHNICAL REPORT

External Grant Ward Number G12AP20093

Title

# Spatial and Temporal Characteristic of Paleoseismic Features in the Southern Terminus of the New Madrid Seismic Zone in Eastern Arkansas

Principal Investigators:

Haydar Al-Shukri and Hanan Mahdi
Arkansas Earthquake Center
University of Arkansas at Little Rock
2801 South University Avenue
Little Rock, AR 72204

Martitia Tuttle and K. Dyer Williams
M. Tuttle & Associates
P.O. Box
Georgetown, ME 04548

7/1/2012 – 5/31/15

## ABSTRACT

Paleoliquefaction investigation of large sand blows was conducted for the purpose of constraining the timing, locations, and magnitudes of paleoearthquakes centered in the study area and identifying and characterizing the fault(s) responsible for these events. This was achieved by conducting (1) detailed ground penetrating radar (GPR) and of sand blows at two sites that occur along a northwest-oriented lineament, (2) paleoseismic investigations at the sites including excavating and logging of sand blows and any related faults and collecting samples for radiocarbon and optically stimulated luminescence (OSL) dating, (3) liquefaction potential analysis using previously collected cone-penetration test (CPT) data to help constrain the magnitude of paleoearthquakes, (4) and analysis of the results in terms of the paleoearthquake history in east-central Arkansas. More specifically we conducted geophysical and paleoliquefaction investigations at two sites, Daytona Beach Northwest (DBNW) site and Nancy-2 North-1 site (Figure 2). The DBNW occur within a northwest-oriented zone of large sand blows and above a bedrock fault identified in seismic reflection profiles collected by the US Geological Survey in 2010. The Nancy-2 North-1 occur within a north-northeast trending shallow fault. Two trenches were excavated at each of these two site after a through GPR surveying to site the location of these trenches.

The two trenches at Daytona Beach Northwest confirm the interpretations of the geophysical data that at least one large sand dike and sand blow formed at this site along the Daytona Beach lineament. Differences in weathering characteristics of the sand blows and sand dikes observed in the trenches at the site suggest that they may have formed during different earthquakes thousands of years apart. The age difference is generally supported by OSL ages of samples collected of the buried soil/sand blow contact in the two trenches. There are large uncertainties associated with the OSL ages but they suggest that the younger sand blow formed about 19 ka and the older sand blow may have formed 5-16 kyr earlier. The geophysical interpretation of numerous GPR profiles at Nancy2 North1 shows a high-angle fault exists at about 1 meter below the sand blow. This observation was confirmed by the two trenches excavated in the fall of 2013. Integrating both trench results and geophysics, it appears that the fault below Nancy2 North1 trends north-northeast, which differs from the northwest trend of the Daytona Beach fault. One scenario interpretation is that Nancy2 North1 is related to Nancy 2 located about 700 m to the south. This is supported by the overlapping dates for Nancy2 and Nancy2-N1 suggesting that the sand blows may have formed about 6000 yr ago.

The analysis of two CPT data collected by the USGS within hundreds meters of both studied sites suggests that earthquakes in the M 6-6.5 range could induce liquefaction in a thick section of sandy sediment below 12.5-13 m and therefore be responsible for the formation of the large sand blows. At this time, the magnitude estimate of M 6-6.5 should be viewed as a minimum value pending further investigations.

## Introduction

A basic assertion of paleoliquefaction studies is that large magnitude earthquakes, ≥ 6, may leave a geological record in the form of liquefaction-related features. Primary among these features are sand blows formed due to the venting of sand and water to the surface as a result of earthquake-induced liquefaction. The presence of sand blows in the geologic record provides an opportunity for estimating the age of prehistoric earthquakes. Employing contemporary dating techniques allows for estimation of the age of individual liquefaction features. By documenting the spatial distribution of similar-age features, the source area of the causative event can be identified. In addition, the area affected by liquefaction and the size distribution of the liquefaction features are indicative of the magnitude of the earthquake. Once the timing, source area, and magnitude of prehistoric earthquakes are determined, the recurrence intervals of large earthquakes can be estimated and used to define the long-term behavior of seismogenic fault zones (Pavlides *et al*., 1999; Tuttle, 2001).

Our understanding of earthquake hazards in the New Madrid seismic zone (NMSZ), the Wabash Valley seismic zone, and now the Marianna area, has profoundly changed as a result of paleoliquefaction investigations. In the NMSZ, careful study of hundreds of sand blows over a large region, as well as fault-related deformation along the Reelfoot scarp and the Bootheel lineament, has led to the development of an earthquake chronology and estimate of a 500-year recurrence time for New Madrid events (e.g., Schweig *et al*., 1992; Tuttle and Schweig, 1995; Kelson *et al.*, 1996; Li *et al.*, 1998; Tuttle, 1999; Tuttle *et al.*, 2002, 2005). More recently, reconnaissance for paleoliquefaction features related to New Madrid seismicity has extended as far north as St. Louis, Missouri, as far west as Batesville, Arkansas, as far east as Union City, Tennessee, and as far south as Madison, Arkansas.

Few modern earthquakes have been recorded in east-central AR; however, its proximity to the New Madrid seismic zone (NMSZ) and the Reelfoot Rift fault system have led some to wonder about the earthquake potential of the region (Figure 1). There are several potential earthquake sources in east-central AR, including the eastern margin of the Reelfoot Rift, the White River fault zone, and the Big Creek fault zone (Fisk, 1944; Krinitzsky, 1950; and Spitz and Schumm, 1997). The eastern Reelfoot Rift margin (ERRM) affects the regional drainage pattern in both the St. Francis basin and the Western Lowlands (Spitz and Schumm, 1997). The rift margin crosses the study area northwest of Marianna and terminates near the White River against a northwest-trending structure related to the Ouachita front (Hildenbrand, 1984). The White River fault zone (WRFZ) is northwest-oriented, controls and deflects local drainages, and breaches and offsets the southern end of Crowley's Ridge at the Marianna Gap (Spitz and Schumm, 1997). Although it appears to be structurally controlled, the Marianna Gap also has been shaped by the Mississippi, St. Francis, and L'Anguille Rivers. The Big Creek fault zone, south of Marianna, parallels the Reelfoot Rift margin and marks the boundary between southward-trending Wisconsin valley-train deposits and southwest-trending Holocene meander-belt deposits (Fisk, 1944; and Krinitzsky, 1950).

During the past ten years, paleoliquefaction studies conducted by this research team near Marianna, AR, located about 80 km south of the southern end of the NMSZ and 70 km southwest of Memphis, TN, led to the discovery of very large sand blows suggesting that large earthquakes were centered in this region 5,000-11,000+ years ago (e.g., Al-Shukri et al., 2006 and 2009; Tuttle et al., 2006). These studies involved identifying sand blows on aerial photographs and satellite images, imaging sand blows and related feeder dikes with ground-penetrating radar (GPR), excavating sand blows to verify their origin, documenting their characteristics, collecting samples for dating, and comparing the size and ages of Marianna sand

blows to those in the NMSZ. Here, we present results of our recent study that involved GPR profiling and paleoseismic trenching at two additional sites in the Marianna area and evaluating scenario earthquakes using liquefaction potential analysis to help constrain magnitude estimates of paleoearthquakes that induced liquefaction in the area.

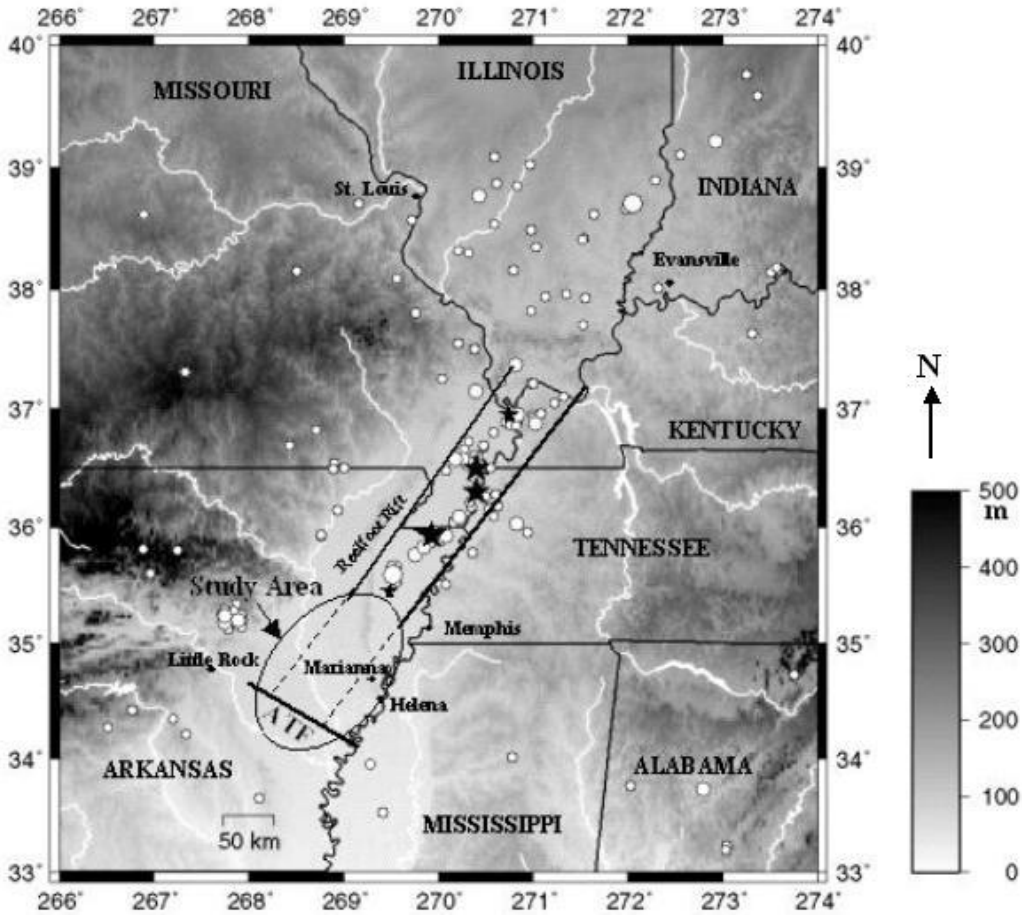


Figure1. Map of the central U.S. showing east-central Arkansas study region (circled) in relation to major structural elements including Reelfoot Rift fault system and Arkansas Transform Fault (ATF, black lines) and seismicity between 1974 and 2005 with magnitudes between 3 and 5.0 (white dots). Large (M>6) historical earthquakes of New Madrid seismic zone within the Reelfoot Rift fault system are depicted as black stars (Modified from Al-Shukri *et al.,* 2006).

## Paleoseismic Investigations

### Daytona Beach Northwest Site

Daytona Beach Northwest (DBNW) is located along a previously recognized northwest-southeast oriented lineament and about 600 m northwest of the original Daytona Beach site (Figure 2.; Tuttle et al., 2006). Although disturbed by agricultural practices, the DBNW site was chosen for study because a large sand blow appeared to have formed along the lineament. Based on observations of sandy soils on the ground surface and in soil pits, we selected an area of 350 m by 200 m for GPR survey in order to map the likely sand blow and to identify its feeder dikes. We collected multiple GPR profiles and created a 3-D image that show a disturbed sediment

boundary about 1-2 meters below the surface suggestive of a paleosol breached by a large sand dike and buried by a large sand blow (Figure 3). We sited two parallel east-west oriented trenches spaced about 25 m apart to cross the large sand dike. Both trenches were about 3 m deep and 18 m long. We logged 9 m of the northern walls of both trenches where the sand dikes and overlying sand blows were exposed (Figures 4 and 5).

In the south trench, we found one very large sand dike about 6 m wide, a buried soil of grayish brown clayey silt that was displaced downward about 1.5 m on the west side of the dike, and a sand blow above the dike and buried soil that was at least 2.4 m thick (Figure 4). The eastern and western margins of the large dike had strikes and dips of N43°W 86°NE and N36°W 84°SW, respectively. The sand dike and related sand blow are composed of reddish brown to tan, massive, medium to fine sand with few small pebbles and clasts of clayey silt. West of the sand dike, the uppermost part of the sand blow is disturbed and overlain by fill including a nail and nylon; whereas, above the dike, the uppermost part of the sand blow is disturbed by plowing. Below the plow zone, the upper 0.5 m of the sand blow is mottled and a few soil lamellae have formed along the eastern margin of the dike.

The degree of weathering suggests that the sand blow is thousands of years old. Unfortunately, no organic samples were found in the paleosol buried by the sand blow to help constrain the maximum age of the sand blow. A charcoal sample (C2) was collected from the plow zone and submitted to Beta Analytic for AMS dating. The sample (Beta - 403853) yielded a modern conventional radiocarbon age (123.3 ± 0.3 percent modern carbon). Two sediment samples (TS-OSL1 and TS-OSL2) were collected of the contact between the buried soil and overlying sand blow and submitted to the U.S. Geological Survey's Optically Stimulated Luminescense (OSL) Laboratory (Figure 4). Analyses were performed on quartz grains using high-resolution gama spectrometry. Samples TS-OSL1 and TS-OSL2 yielded ages of 15,100 ± 4,540 years and 19,600 ± 1,010, respectively (Table 1). The two ages overlap between 18,590 - 19,640 ka. If these ages represent close maximum ages, the sand blow formed about 19 ka.

In the north trench, we also found one very large sand dike about 4.5 m wide, a buried soil of grayish brown clayey silt that was displaced downward about 1.1 m on the west side of the dike relative to the buried soil on the east side of the dike (2.1 m relative to the ground surface), and a sand blow above the dike and buried soil that ranged from 1.1-2.4 m thick (Figure 5.). As measured across the floor of the trench, the eastern margin of the large dike has a strike and dip of N36°W 86°NE. The overall trend of the eastern margin of the large sand dike exposed in the two trenches is N41°W.

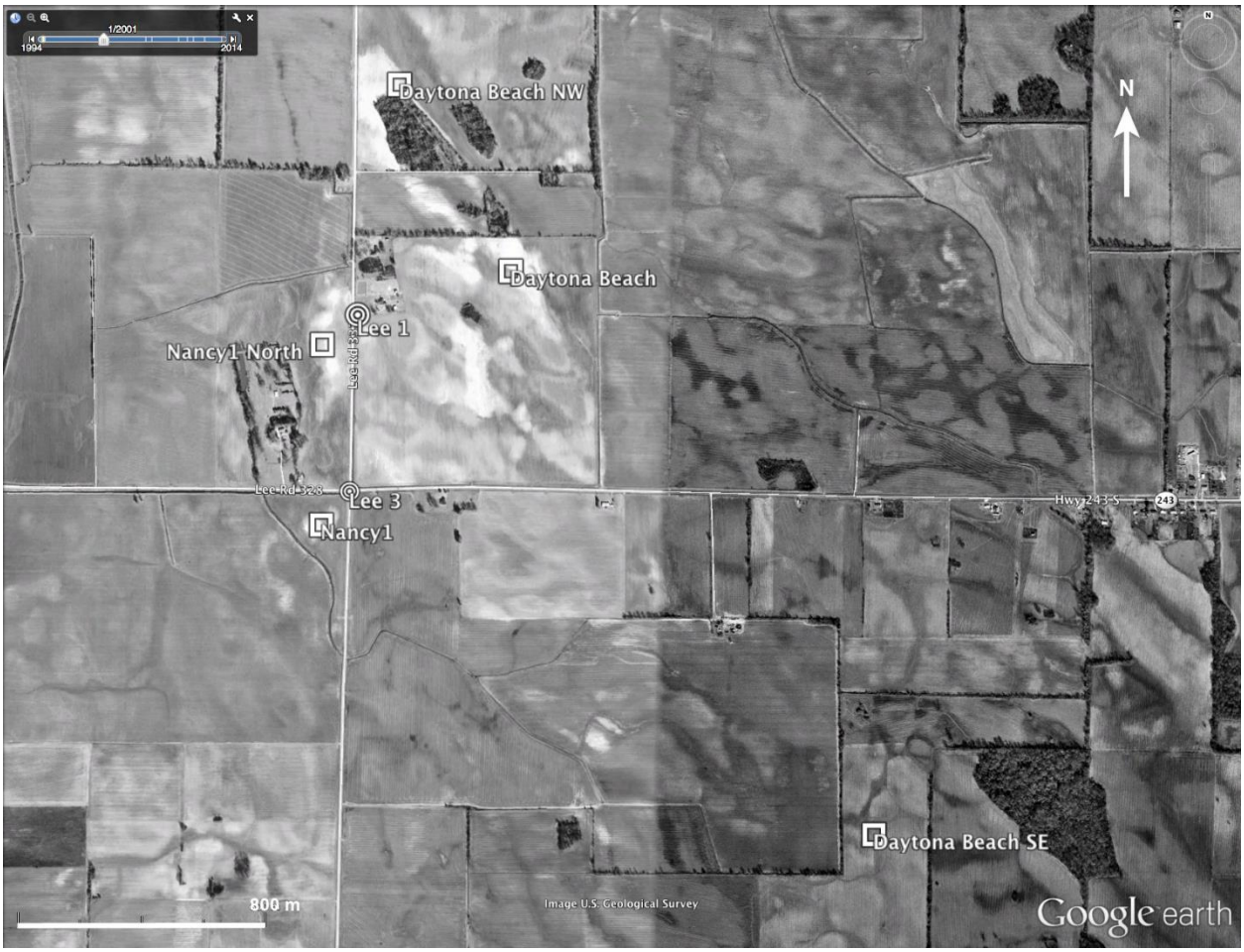


Figure 2. Google Earth satellite image acquired January 2001 of study area. Paleoseismic investigations, including GPR surveys and paleoseismic trenching, at Daytona Beach NW and Nancy2-North sites are presented in this report. Locations of paleoseismic study sites are indicated by white squares and cone penetration test sites are indicated by white concentric circles.

The sand dike and related sand blow are composed of reddish brown to tan, massive, fine sand with few small pebbles, granules, and clasts of clayey silt. Flow structure was observed in the sand blow above the sand dike. The uppermost part (20-50 cm) of the sand blow is disturbed by plowing. Below the plow zone, the upper 0.5 m of the sand blow is mottled. Soil lamellae have formed at the base of the sand blow above the buried soil and along both margins of the dike, and is especially well developed along the eastern margin. Two soft-sediment faults within a meter and subparallel to the eastern dike margin crosscut soil lamellae. There are thickness differences but no vertical offsets of lamellae across the faults suggesting strike-slip movement. Discontinuous dikes of loose fine sand containing granules intrude the soil lamellae along the soft-sediment faults.

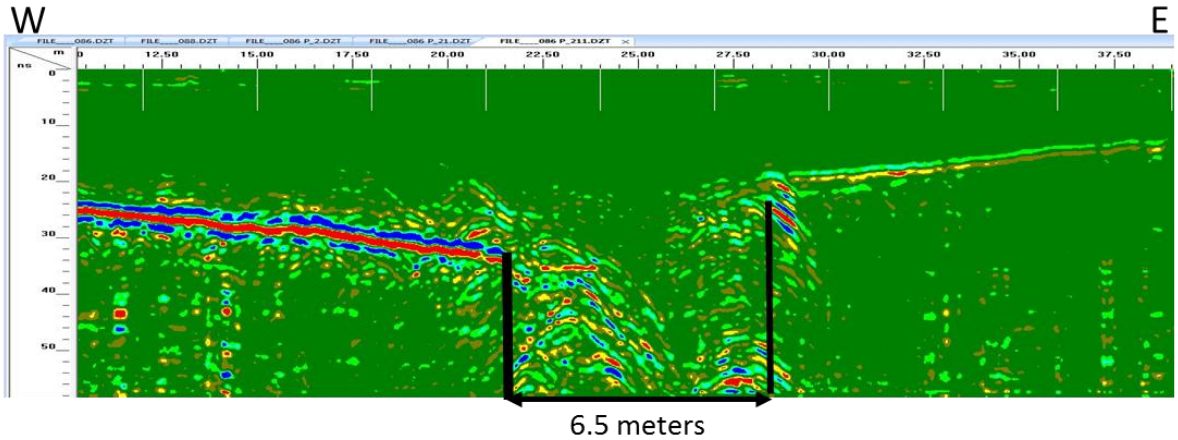


Figure 3. GPR data from DBNW site shows anomalies related to sand blow and related feeder dike. Red and blue color bands represent the contact between the sand blow and silt loam (old surface). The dike location is shown between the two vertical black lines.

The degree of weathering, including formation of a thick section of soil lamellae, suggests that the sand blow is thousands to tens of thousands of year old. Unfortunately, no organic samples were found in the paleosol buried by the sand blow to help constrain the maximum age of the sand blow. Two sediment samples (TN-OSL1 and TN-OSL2) were collected of the contact between the buried soil and overlying sand blow and submitted to the U.S. Geological Survey's OSL laboratory (Figure 5.). Similar analyses were performed on these samples collected in the south trench. Samples TN-OSL1 and TN-OSL2 yielded ages of 32,500 ± 1,880 years and 24,400 ± 1,790, respectively (Table 1). Although the samples were collected of the same sand blow/soil contact and only 60 cm apart, the age of the two samples do not ages overlap with each other or with the ages of samples collected in the southern trench. Furthermore, they do not overlap with any of the radiocarbon ages or OSL ages previously determined at the Daytona Beach, Daytona Beach SE, or Nancy 2 sites also determined by the same laboratory, though the age of TN-OSL1 (32,500 ± 1,880 yr) comes close to overlapping with the age of the older (38,000 ± 3,000 yr) and very weathered sand blow at Daytona Beach SE. Perhaps the older sand blows at Daytona Beach North and Daytona Beach SE formed during the same event about 35 ka.

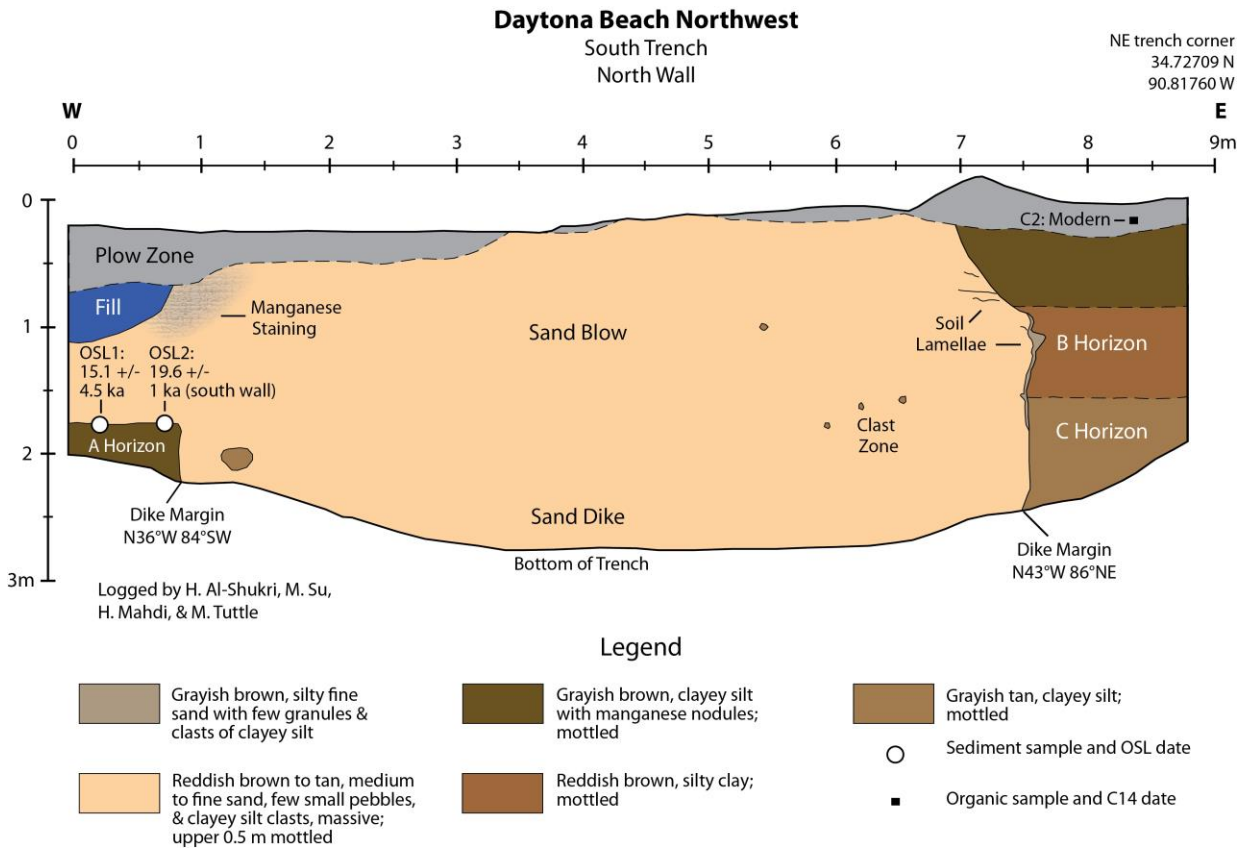


Figure 4. Log of the north wall of the south trench at site DBNW.

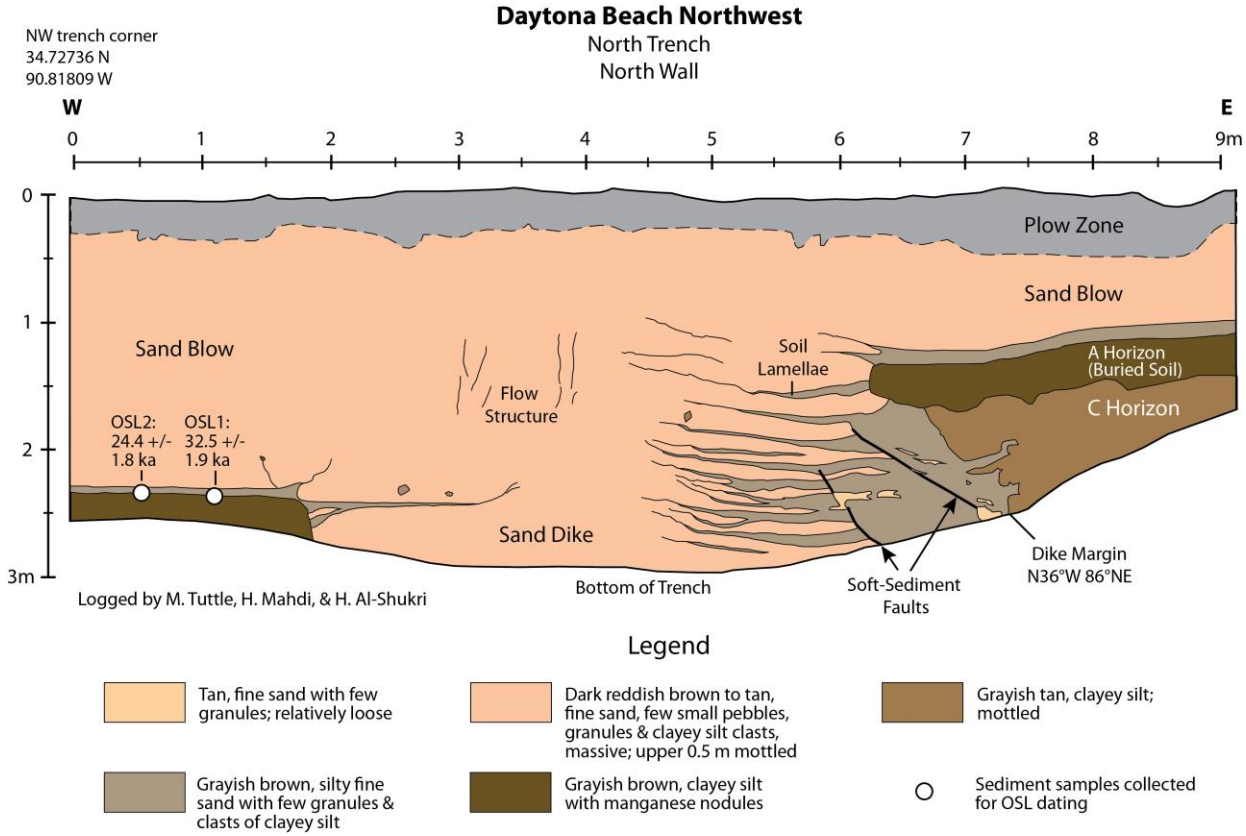


Figure 5. Log of the north wall of the north trench at site DBNW.

Table 1: Results of Optically Stimulated Luminescense Dating

| Sample Information | % Water Content[a] | K (%)[b] | U (ppm)[b] | Th (ppm)[b] | Total Dose (Gy/ka)[d] | Equivalent Dose (Gy) | n[e] | Scatter[f] | Age (yrs)[g] |
|---|---|---|---|---|---|---|---|---|---|
| DBN TN-OSL1 | 12 (26) | 1.34 ± 0.03 | 1.30 ± 0.04 | 4.50 ± 0.14 | 2.03 ± 0.06 | 65.9 ± 3.34 | 3 (15) | 29% | 32,500 ± 1,880 |
| DBN TN-OSL2 | 12 (21) | 1.01 ± 0.04 | 0.91 ± 0.11 | 2.94 ± 0.26 | 1.54 ± 0.08 | 37.5 ± 1.97 | 2 (15) | 41% | 24,400 ± 1,790 |
| DBN TS-OSL1 | 12 (33) | 1.30 ± 0.03[c] | 0.90 ± 0.03[c] | 3.56 ± 0.18[c] | 1.82 ± 0.05 | 27.5 ± 0.42 | 2 (14) | 42% | 15,100 ± 4540 |
| DBN TS-OSL2 | 13 (21) | 1.25 ± 0.03[c] | 0.60 ± 0.02[c] | 2.80 ± 0.14[c] | 1.70 ± 0.04 | 33.3 ± 1.51 | 2 (7) | 33% | 19,600 ± 1,010 |
| DBW T1-OSL1 | 10 (25) | 2.80 ± 0.05 | 1.30 ± 0.14 | 5.61 ± 0.43 | 3.50 ± 0.13 | 21.1 ± 1.07 | 2 (13) | 42% | 6,030 ± 380 |
| DBW T1-OSL2 | 12 (30) | 2.97 ± 0.05 | 1.57 ± 0.13 | 6.69 ± 0.42 | 3.75 ± 0.12 | 61.9 ± 6.27 | 3 (15) | 24% | 16,500 ± 1,750 |
| DBW T1-OSL3 | 12 (30) | 1.61 ± 0.04 | 1.48 ± 0.09 | 5.32 ± 0.27 | 2.37 ± 0.07 | 76.6 ± 10.9 | 1 (3) | 37% | 32,300 ± 4,680 |
| DBW T2-OSL1 | 8 (27) | 1.32 ± 0.03[c] | 0.80 ± 0.02[c] | 3.40 ± 0.17[c] | 1.83 ± 0.05 | 104 ± 13.2 | 1 (3) | 22% | 56,700 ± 7,360 |

[a]Field moisture, with figures in parentheses indicating the complete sample saturation %. Ages calculated using 25% of the saturated moisture (i.e. 12 (26) = 26 * 0.25 = 6).
[b]Analyses obtained using high-resolution gamma spectrometry (Ge detector).
[c]Analyses obtained using inductively coupled plasma mass spectrometry (ICP-MS). All errors were obtained with calibration standards.
[d]Includes cosmic doses and attenuation with depth calculated using the methods of Prescott and Hutton (1994). Cosmic doses varied from 0.16 to 0.18 Gy/ka.
[e]Number of replicated equivalent dose (De) estimates used to calculate the equivalent dose. Figures in parentheses indicate total number of measurements included in calculating the represented equivalent dose and age using the minimum age model (MAM). Single grain and single aliquot readings are combined.
[f]Defined as "over-dispersion" of the De values. Obtained by the "R" factor program. Values >35% are considered to be poorly bleached or mixed 'sediments.
[g]Dose rate and age for fine-grained 250-180 microns quartz (except for T2S1 at 150-90 microns). Exponential + linear fit used on equivalent dose, errors to one sigma.

One interpretation is that the sand blows observed in the two trenches formed during two different earthquakes separated by thousands of years, perhaps ten thousand years. The sand blow in the north trench would be the older of the two sand blows as suggested by the development of soil lamellae at the base of the sand blow and along the margin of the dike. An older age is supported by the OSL ages, though there are large uncertainties associated with the ages. The soft-sediment faults and intruded sand dikes that crosscut the soil lamellae in the northern sand blow suggest a subsequent event large enough to induce liquefaction thousands of years after the sand blow formed. Perhaps faulting and liquefaction occurred at the same time as the southern sand blow formed. To verify that there are two generations of sand blows and to further assess their temporal relationship, a third trench is needed between the north and south trenches.

An alternate interpretation is that the sand blows observed in the two trenches are one in the same and that the difference in soil lamellae development is due to local variations in translocation of fines down section and that the OSL ages are almost meaningless for dating burial of the paleosol by the large sand blow. In this scenario, the soft-sediment faults and sand dikes that crosscut the soil lamellae in the north trench would still indicate a subsequent event.

## Nancy-2 North-1 Site

The site located about 650 m to the west-southwest of the original Daytona Beach site (Figure 2). The likely scenario is that the liquefaction features at this site is the northern extension of those at Nancy-2 site located about 700 m to the south (Al-Shukri et. al, 2005, 2006). Similar to the DBNW site, the surface expression of Nancy-2 North-1 is about 200m by 200m fine to medium grain sand blow that was precision leveled during the fall of 2014. This farming practice most likely modified the surface expression of the sand blow. Based on the surface expression of the sand blow and exploratory soil pits, we selected an area about 100m (N-S) by 150m (E-W) for detailed GPR surveying. Several GPR profiles we collected and analyzed. Most of these profiles were surveyed in the E-W direction. We also surveyed a few in the N-S direction. Based on our experience of analyzing hundreds of GPR profiles in the area, the GPR data clearly showed that the continuity of the contact between the sand and the silt had been disturbed in at least one location. Figure 6 is an example of E-W GPR profile showing a clear disruption to the sand-silt contact at a depth of about 1 meter.

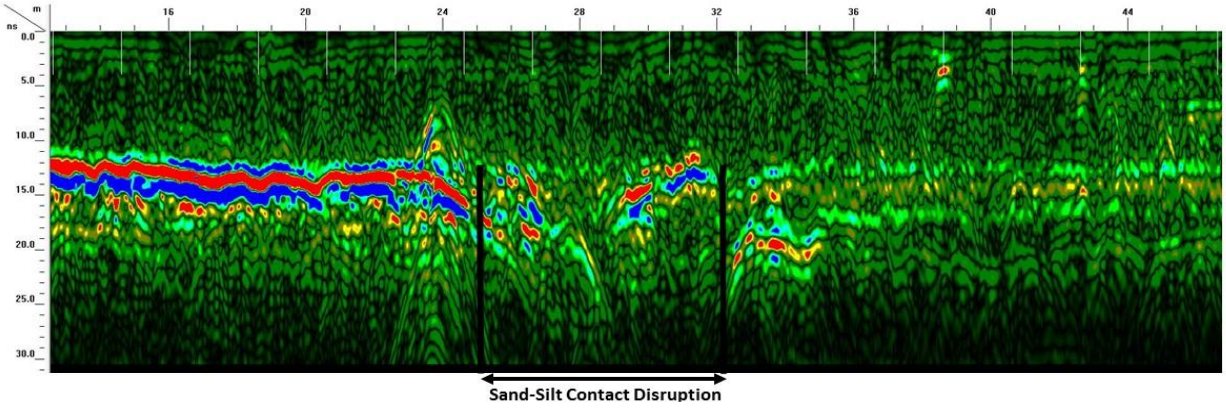


Figure 6. W-E oriented GPR profile indicating subsurface soil disruption at Nancy-2 N-1 site.

To map this disruption at the surface, several E-W GPR profiles (parallel to the one in Figures 6 and 7) were collected and analyzed. We also sited the locations of two E-W trenches to study the nature of this disruption and to collect samples for dating (Figures 8 and 9). The southern trench located between 34.72059N 90.82072W (west end) and 34.72058N 90.82032W (east end) and having a length of 36 meters. Both trenches show a small displacement high-angle fault in the silt that was precisely corresponded with the disruption observed in the GPR profiles.

Figure 7. Nancy2-N1 site – GPR data (green lines), trench locations (black lines), and surface projection of the fault (small arrows)

The result of the trenches and the GPR profiles are summarized in Figure 7 which indicates that the fault strikes in the north-northeast direction. This is different than the northwest orientation of the Triple-Crown – DB – DBNW structure. Combining this with the OSL (Table 1) dating results, two possible scenarios may explain this observation. The first is that the observed fault is a secondary feature to the major DB structure and the second is that it represents different episode of earthquakes and faulting. OSL sample DBW T1-OSL date (~6000 yr) overlaps with Radiocarbon dating of charcoal collected from Nancy 2 trench (Al-Shukri et. al, 2005). If these two sand blows are related to the same structure, a possibility that they were created by different earthquake(s) episode than the one generated DBNW. This further complicates the structural setting of the area and more dating data is need to help resolve this complexity.

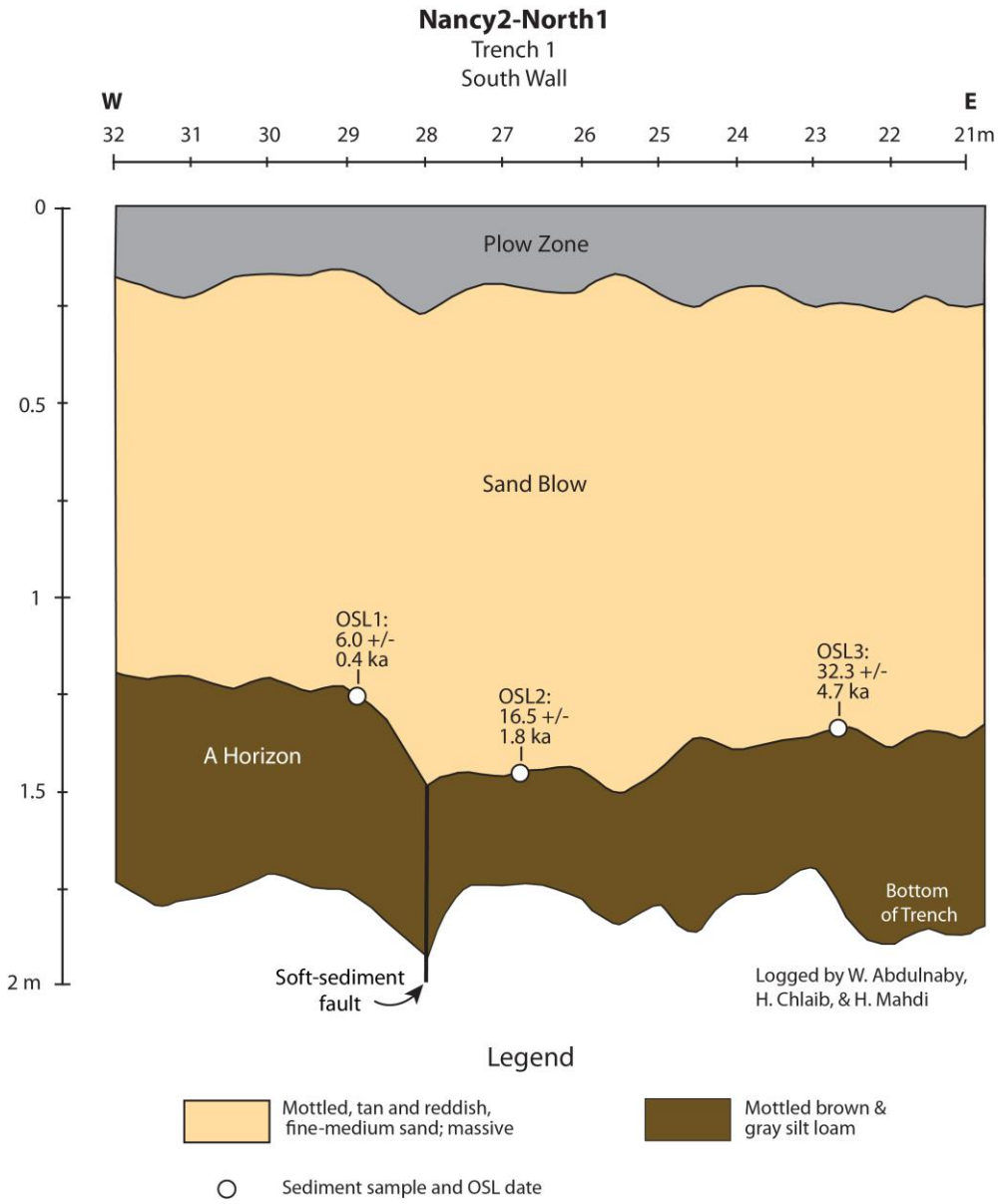


Figure 8. Portion of log of the south wall of trench 1 at site Nancy2-North1 that shows the high-angle fault, sand blow, and OSL dating results of the buried soil.

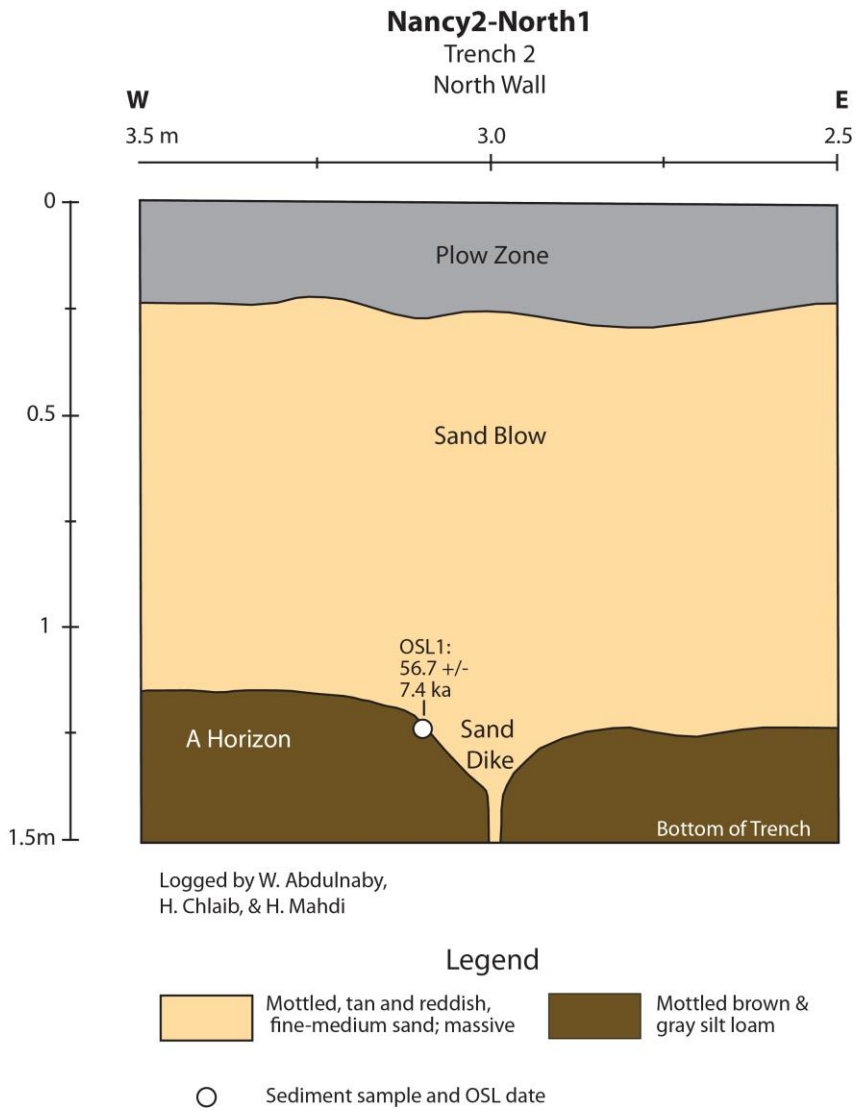


Figure 9. Portion of log of the north wall of trench 2 at site Nancy2-North1 that shows the feeder dike and related sand blow, and OSL dating results of the buried soil.

## Evaluation of Scenario Earthquakes

### Methodology

In order to help constrain the magnitude of the paleoearthquakes, we determined whether or not various scenario earthquakes (e.g., moment magnitude, **M,** 5.5, 6.0, and 6.5 earthquakes at distances of 5 km and 10 km) are likely to induce liquefaction in the vicinity of the study sites. The scenario earthquakes were evaluated using the cyclic stress method, also known as the simplified procedure, for assessing liquefaction potential (e.g., Seed and Idriss, 1971 and 1982; Youd et al., 2001; Cetin et al., 2004; Idriss and Boulanger, 2004; Moss et al., 2006; Robertson, 2004 and 2009). We evaluated scenario earthquakes at distances of 5 km and 10 km because (1) the Daytona Beach and Nancy2 sand blows are thought to occur immediately above the active faults that produced paleoearthquakes in the area and (2) seismicity in the Mississippi Embayment typically occurs between 5-10 km depth. Two water table depths (1.5 m and 5 m) were considered in the analysis since the water table may have been deeper at the time of the paleoearthquakes than it was in the Late Holocene.

In order to calculate the liquefaction potential of a site, the depth and relative density of sandy soils or sediment must be known. This information was provided by *in situ* geotechnical testing performed by the U.S. Geological Survey in 2004 (Figures 10 and 11). Cone penetration test (CPT) data, including measurements of cone tip resistance and sleeve friction were collected at several sites in the area. We used the CPT data collected at sites Lee 1 and 3 in the analysis (Figure 2).

Stress-normalized cone resistance and normalized sleeve friction were used to calculate the CPT material index ($I_c$) as follows:

$$I_c = \sqrt{[3.47 - \log Q_{tn}]^2 + [1.22 + \log F_r]^2}$$

where $Q_{tn}$ = stress-normalized cone resistance and $F_r$ = normalized sleeve friction (Robertson, 2004). These parameters are derived from the cone penetrometer readings according to the following relations:

$$Q_{tn} = \frac{(q_t - \sigma_{vo})/\sigma_{atm}}{(\sigma_{vo}'/\sigma_{atm})^n}$$

$$F_r\ (\%) = 100 \cdot \frac{f_s}{(q_t - \sigma_{vo})}$$

where $\sigma_{vo}$ = total vertical overburden stress, $\sigma_{vo}'$ = effective vertical stress, and $\sigma_{atm}$ = a reference stress equal to atmospheric pressure (1 atm ≈ 1 bar ≈ 100 kPa) (Robertson and Wride, 1998; and Zhang et al., 2002). The exponent n is a stress-normalizing parameter that varies with soil type (i.e., taken as n = 1 in clay and decreases with coarseness to about 0.75 in silt and about 0.5 ± 0.2 in clean sand). Generally, soils that are susceptible to cyclic liquefaction are sandy materials identified by $I_c < 2.6$. Therefore, sediment likely to be susceptible to liquefaction occurs below 13 m at Lee 1 and below 12.5 m at Lee 3.

The fines content (FC in %) was estimated from the CPT material index $I_c$ as follows:

For $I_c < 1.64$ FC (%) = 0

For $1.64 \leq I_c \leq 3.5$: FC (%) = $1.75\,(I_c)^{3.25} - 3.7$

For $I_c > 3.5$ FC (%) = 100

A correction for fines content was applied to give the equivalent value of stress-normalized cone resistance for clean sands according to (Robertson and Wride, 1998):

$$(Q_{tn})_{cs} = K_c \cdot Q_{tn}$$

where the correction factor $K_c$ was obtained from:

For $I_c \leq 1.64$: $K_c = 1.0$

For $I_c > 1.64$: $K_c = -0.403 I_c^4 + 5.581 I_c^3 - 21.63 I_c^2 + 33.75 I_c - 17.88$

<u>Calculating CRR:</u> For clean sands, the CRR is expressed by the following equations for an earthquake moment-magnitude of 7.5 (Youd et al., 2001; Robertson and Wride, 1998):

For $(Q_{tn})_{cs} < 50$: $$CRR_{7.5} = 0.833\left[\frac{(Q_{tn})_{cs}}{1000}\right] + 0.05$$

For $50 \le (Q_{tn})_{cs} < 160$ $$CRR_{7.5} = 93\left[\frac{(Q_{tn})_{cs}}{1000}\right]^3 + 0.08$$

CRR for magnitudes other than 7.5 is calculated by multiplying $CRR_{7.5}$ by the appropriate Magnitude Scaling Factor (MSF), which is given by the expression:

MSF = (10)^2.24/M^-3.3

<u>Calculating CSR:</u> Peak ground accelerations are estimated for the scenario earthquakes using regionally appropriate attenuation relations. We selected the Referenced Empirical GMPE of Atkinson, (A08') in Atkinson and Boore (2010) to calculate peak ground accelerations (amax). Cyclic stress ratios (CSR) generated by scenario earthquakes were calculated using the following expression:

$$\mathrm{CSR}_{7.5} = \frac{\tau_{ave}}{\sigma'_{vo}} = 0.65 \cdot \left(\frac{a_{max}}{g}\right) \cdot \left(\frac{\sigma_{vo}}{\sigma'_{vo}}\right) \cdot r_d \cdot \frac{1}{\mathrm{MSF}}$$

where ($a_{max}$/g) = PGA = peak ground acceleration, $\sigma_{vo}$ and $\sigma_{vo}'$ are the total and effective vertical overburden stresses, respectively, and $r_d$ is a stress reduction coefficient (Youd et al., 2001). The $CSR_{7.5}$ represents the normalized shear stress ($\tau_{ave}/\sigma_{vo}'$) induced in the soil by the earthquake and commonly referenced to a benchmark case with **M** 7.5.

<u>Probability of Liquefaction and Factor of Safety:</u> Following the computations of the cyclic stress ratio (CSR) and the cyclic resistance ratio (CRR), liquefaction potential for each depth interval was determined by plotting computed cyclic stress ratio (CSR) and cyclic resistance ratio (CRR) versus depth. The results are shown for the different scenario earthquakes in Appendix A. If the value for sandy soil plots to the left of the cyclic resistance ratio (CRR) curve, the soil is likely to liquefy. Conversely, if the value plots to the right of the CRR curve, liquefaction is considered unlikely.

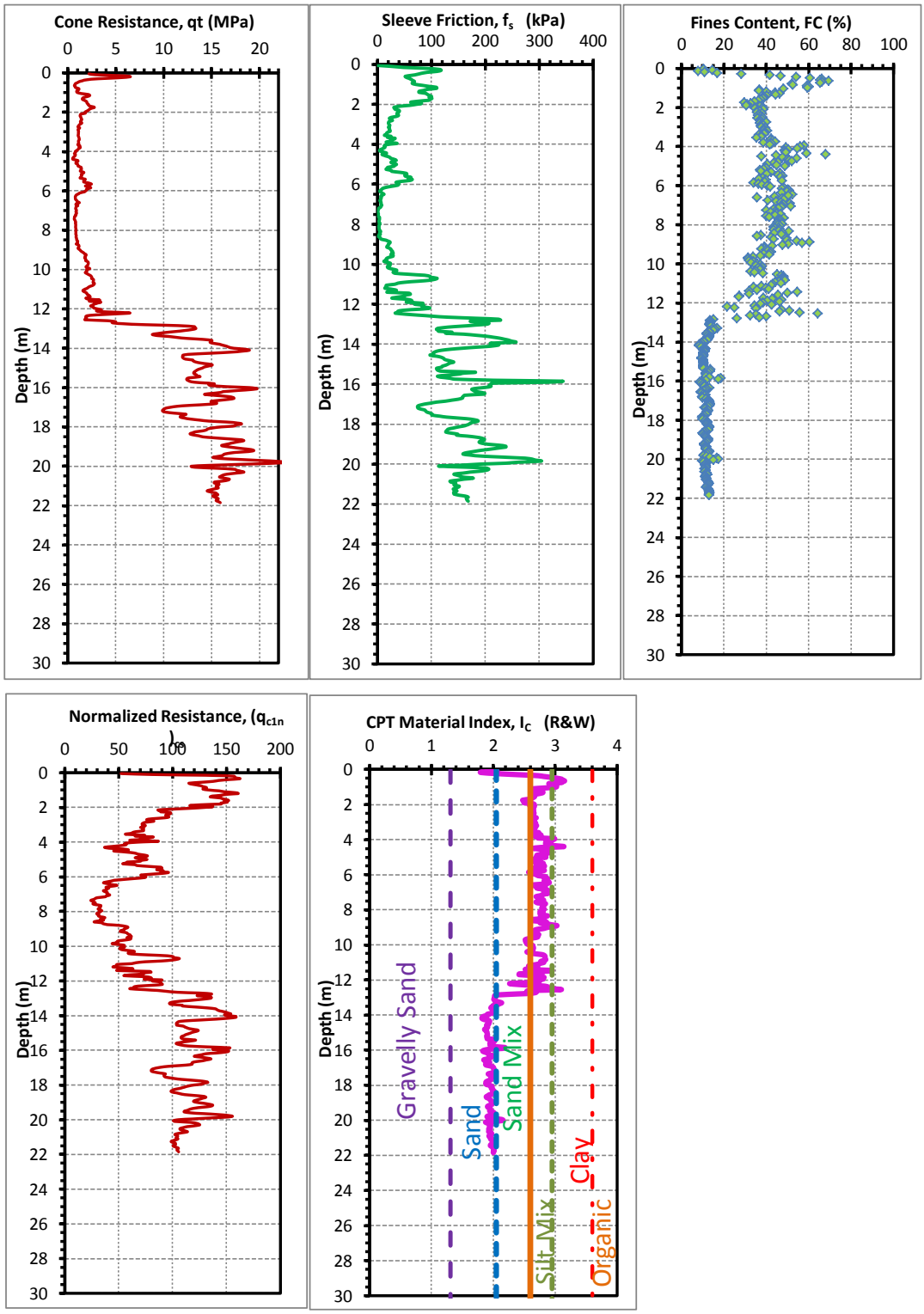


Figure 10. Results of CPT at site Lee 1 southwest of Marianna, Arkansas (from USGS - Holder and Noce, Personal Communication; see Figure 2 for the site location).

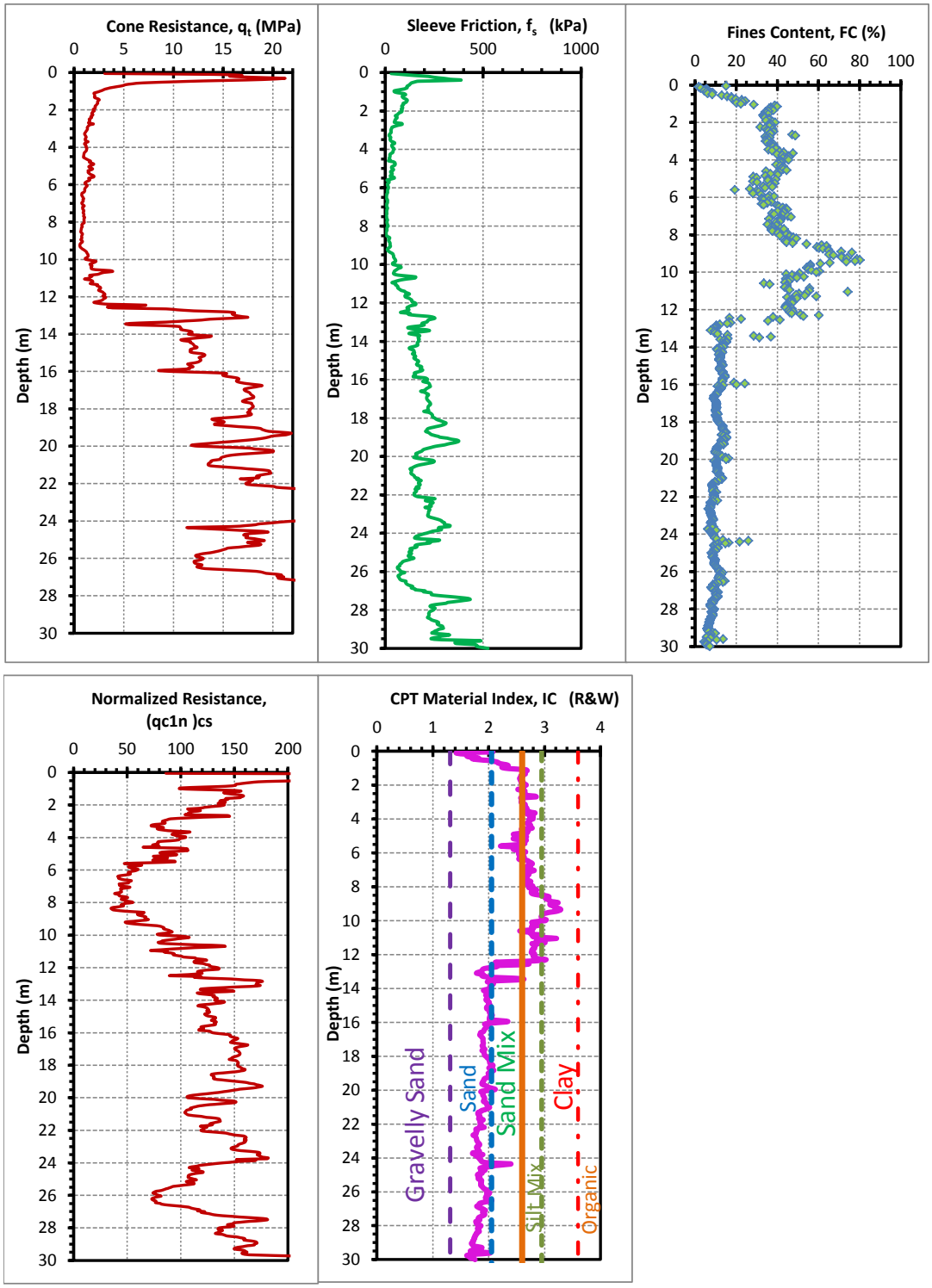


Figure 11. Results of CPT at site Lee 3 southwest of Marianna, Arkansas (from USGS - Holzer and Noce; see Figure 2 for the site location).

We also calculate the probability of liquefaction, $P_L$, and the factor or safety, FS, for each depth interval using the equations (Juang et al., 2000):

$P_L$= 1/(1+(Fs/1.0)^3.34 and

$F_s$= CRR/CSR

The FS was plotted for each depth interval. The results are shown for the different scenario earthquakes in Appendix A. Sandy soils below 13 m at Lee 1 and below 12.5 m at Lee 3 (identified with pink shading) with a factor of safety less than 1 are likely to liquefy.

**Results**

The results of liquefaction potential analysis for scenario earthquakes of **M** 5.5, 6.0, and 6.5 at distances of 5 and 10 km and for water-table depths of 1.5 and 5 m are presented in Appendix A and summarized in Tables 2 and 3. In appendix A, the results are shown as diagrams of CRR and CSR with depth and FS with depth. Here we review the results.

Considering the site Lee 1 first with a water-table depth of 1.5 m, the analysis predicts that very little of the sediment below 13 m would liquefy during a **M** 5.5 earthquake even if it were only 5 km away. The analysis suggests that a **M** 6.0 earthquake at a distance of 5 km would liquefy much of sediment below 13 m; but a **M** 6.0 at a distance of 10 km would not. In contrast, a **M** 6.5 earthquake whether at 5 and 10 km distance would likely liquefy almost the entire sandy section below 13 m. Very similar results were obtained for a water-table depth of 5 m.

Table 2. Results of Paleoliquefaction Analysis for site Lee 1

| **Moment Magnitude** | **Distance (km)** | **Liquefaction[1] Water Table 1.5 m** | **Liquefaction[1] Water Table 5 m** |
|---|---|---|---|
| 5.5 | 5 | N | N |
| 5.5 | 10 | N | N |
| 6.0 | 5 | L | L |
| 6.0 | 10 | N | N |
| 6.5 | 5 | L | L |
| 6.5 | 10 | L | L |

1. L = liquefaction likely; N = liquefaction not likely

Table 3. Results of Paleoliquefaction Analysis for Site Lee 3

| **Moment Magnitude** | **Distance (km)** | **Liquefaction[1] Water Table 1.5 m** | **Liquefaction[1] Water Table 5 m** |
|---|---|---|---|
| 5.5 | 5 | N | N |
| 5.5 | 10 | N | N |
| 6 | 5 | L | L |
| 6 | 10 | N | N |
| 6.5 | 5 | L | L |
| 6.5 | 10 | L | L |

1. L = liquefaction likely; N = liquefaction not likely

Considering the site Lee 3 with a water-table depth of 1.5 m, the analysis predicts that very little of the sediment below 12.5 m would liquefy during a **M** 5.5 earthquake if it were 5 km away and no sediment would liquefy if the earthquake were 10 km away. The analysis suggests that a **M** 6.0 earthquake at a distance of 5 km would liquefy much of sediment below 12.5 m; but a **M** 6.0 at a distance of 10 km would not. Similar to the analysis for Lee 1, a **M** 6.5 earthquake, whether at 5 and 10 km distance, would likely liquefy almost the entire sandy section below 12.5 m. Very similar results were obtained for a water-table depth of 5 m.

In conclusion, the analysis suggests that an earthquake of **M** 5.5 would produce little if any liquefaction at the CPT sites whether the water table was at 1.5 m or 5 m depth; whereas, an earthquake of **M** 6 at a distance of 5 km or a **M** 6.5 at 10 km is likely to induce liquefaction in much of the sandy sediment below 12.5-13 m regardless of the water-table depth (1.5 m or 5 m).

## Conclusions

Our observations in two trenches at Daytona Beach Northwest confirm the interpretations of the geophysical data that at least one large sand dike and sand blow formed at this site along the Daytona Beach lineament. Differences in weathering characteristics of the sand blows and sand dikes observed in the trenches at the site suggest that they may have formed during different earthquakes thousands of years apart. The age difference is generally supported by OSL ages of samples collected of the buried soil/sand blow contact in the two trenches. There are large uncertainties associated with the OSL ages but they suggest that the younger sand blow formed about 19 ka and the older sand blow may have formed 5-16 kyr earlier. Soft-sediment faults and sand dikes that crosscut soil lamellae in the more weathered and likely older sand dike may have formed at the same time as the less weathered sand blow and dike in the nearby trench. Additional trenching is needed at this site to search for organic samples for radiocarbon dating to gain better control on the age estimates of the liquefaction features and to further explore the relationship of the liquefaction features observed in the two trenches.

The geophysical interpretation of numerous GPR profiles at Nancy2 North1 shows a high-angle fault exists at about 1 meter below the sand blow. This observation was confirmed by the two trenches excavated in the fall of 2013. Integrating both trench results and geophysics, it appears that the fault below Nancy2 North1 trends north-northeast, which differs from the northwest trend of the Daytona Beach fault. One scenario interpretation is that Nancy2 North1 is related to Nancy 2 located about 700 m to the south. This is supported by the overlapping dates for Nancy2 and Nancy2-N1 suggesting that the sand blows may have formed about 6000 yr ago.

We evaluated scenario earthquake using liquefaction potential analysis in order to estimate the magnitude of earthquakes that produced the large sand blows in our study area. In the analysis, we used CPT data collected by the U.S. Geological Survey within several hundreds of meters of the Daytona Beach and Nancy 2 liquefaction sites. Given that many of the Daytona Beach sand blows and the Nancy 2 sand blows appear to have formed immediately above the active faults and that seismicity typically occurs between 5-10 km depth in the Mississippi Embayment, we evaluated **M** 5.5, 6.0, and 6.5 earthquakes at distances of 5 km and 10 km. Our analysis suggests that earthquakes in the **M** 6-6.5 range could induce liquefaction in a thick section of sandy sediment below 12.5-13 m and therefore be responsible for the formation of the large sand blows. At this time, the magnitude estimate of **M** 6-6.5 should be viewed as a minimum value pending further investigations.

## References

Al-Shukri H. J., Robert E. Lemmer, H. H. Mahdi, and J. B. Connelly (2005). Spatial and Temporal Characteristics of Paleoseismic Features in the Southern Terminus of the New Madrid Seismic Zone in Eastern Arkansas, *Seismo. Research Lett.*. 76, 502-511.

Al-Shukri, H., H. H. Mahdi, and M. Tuttle (2006). Three- Dimensional Imaging of Earthquake-induced Liquefaction Features with Ground Penetrating Radar near Marianna, Arkansas, *Seismo. Res. Lett.*, 77, 505-513.

Al-Shukri, H., H. H. Mahdi, Al-Kadi, O, and M. Tuttle (2009). Spatial and Temporal Characteristic of Paleoseismic Features in the Southern Terminus of the New Madrid Seismic Zone in Eastern Arkansas, USGS Technical Report 07HQGR0069, 24p.

Atkinson, G.M., and D.M. Boore, "Modifications to Existing Ground Motion Prediction Equations in Light of New data," *Bull. Seismic Soc. Am. (final version).* Dec. 2, 2010.

Cetin, K.O., et al., "Standard Penetration Test-Based Probabilistic and Deterministic Assessment of Seismic Soil Liquefaction Potential," *Journal of Geotechnical and Geoenvironmental Engineering,* American Society of Civil Engineers, 1314-1340, 2004.

Fisk, H. N. (1944). Geological investigation of the alluvial valley of the lower Mississippi River, Mississippi River Commission, Vicksburg, MS, 78 p.

Hildenbrand, T. G. (1984). Rift structure of the northern Mississippi embayment from the analysis of gravity and magnetic data, *in* Gori, P. L., and Hays, W. W., eds, Proceedings of the Symposium on "The New Madrid seismic zone," *U.S. Geol. Surv. Open-File Report 84-770*, p. 168-203.

Idriss, I.M., and R.W. Boulanger, "Semi-Empirical Procedures for Evaluating Liquefaction Potential during Earthquakes," *Proceedings 11th International Conference Soil Dynamics and Earthquake Engineering, v. 1,* Elsevier, Berkeley, CA, 2004.

Juang, C.H., and T. Jiang, "Assessing Probablistic Methods for Liquefaction Potential Evaluation. Soil Dynamics and Liquefaction 2000," *(Proceedings GeoDenver), GSP 107,* American Society of Civil Engineers, Reston, VA, 2000.

Kelson, K.I., G.D. Simpson, R.B. VanArsdale, J.B. Harris, C.C. Haradan, and W.R. Lettis (1996). Multiple Holocene earthquakes along the Reelfoot fault, central New Madrid seismic zone, *Journal of Geophysical Research*, v. 101, n. B3, p. 6151-6170.

Krinitzsky, E. L. (1950). Geological investigation of faulting in the lower Mississippi Valley, *U.S. Army Corps of Engineers Waterways Experiment Station, Tech. Memorandum 3-311*, 50 p.

Li, Y., E.S. Schweig, M.P. Tuttle, and M.A. Ellis (1998). Evidence for large prehistoric earthquakes in the northern New Madrid seismic zone, central United States, *Seismological Research Letters*, v. 69, n. 3, p. 270-276.

Moss, R.E.S., et al., "CPT-based Probablistic and Deterministic Assessment of in-situ Seismic Soil Liquefaction Potential," *Journal of Geotechnical and Geoenvironmental Engineering*, 132(8):1032-1051, 2006.

Pavlides, S.B., P. Zhang, D. Pantosti (1999). Earthquake, active faulting, and paleoseismic studies for the reconstruction of the seismic history of faults, Tectonophysics 308, vii-x.

Robertson, P.K., and C.E. Wride (Fear), "Evaluating Cyclic Liquefaction Potential using the Cone Penetration Test," *Canadian Geotechnical Journal*, 35(3):442-459, 1998.

Robertson, P.K., "Evaluating Soil Liquefaction and Post-Earthquake Deformations using the CPT, Geotechnical and Geophysical Site Characterization, v.1," *(Proceedings ISC-2, Porto),* Millpress, Rotterdam, 2004.

Robertson, P.K., "Interpretation of Cone Penetration Tests: a Unified Approach," *Canadian Geotechnical Journal*, 46(11):1335-1355, 2009.

Seed, H.B., and I.M. Idriss, "Simplified Procedure for Evaluating Soil Liquefaction Potential," *Journal of the Soil Mechanics and Foundations Division (American Society of Civil Engineers*), 97(SM9):1249-1273, 1971.

Seed, H.B. and I.M. Idriss, "Ground Motions and Soil Liquefaction during Earthquakes," Earthquake Engineering Research Institute, Berkeley, CA, 1982.

Schweig, III, E.S., F. Shen, L.R. Kanter, E.A. Luzietti, R.B. VanArsdale, K.M. Shedlock, and K.W. King (1992). Shallow seismic reflection survey of the bootheel lineament area, southeastern Missouri, *Seismological Research Letters*, v. 63, n. 3, p. 285-295.

Spitz, W. J., and S. A. Schumm (1997). Tectonic geomorphology of the Mississippi Valley between Osceola, Arkansas and Friars Point, Mississippi, *Engineering Geology* 46, 259-280.

Tuttle, M.P. (1999). Late Holocene earthquakes and their implications for earthquake potential of the New Madrid seismic zone, central United States, Ph.D. dissertation, University of Maryland, 250 p.

Tuttle, M. P., Al-Shukri, H, and Mahdi, H. (2006). Very large earthquakes centered southwest of the New Madrid seismic zone 5,000-7,000 years ago, *Seismological Research Letters*, v. 77, n. 6, p. 664-678.

Tuttle, M. P. (2001). The use of liquefaction features in paleoseismology: Lessons learned in the New Madrid seismic zone, central United States, Journal of Seismology, v. *5*, p. 361-380.

Tuttle, M.P. and E.S. Schweig (1995). Archeological and pedological evidence for large prehistoric earthquakes in the New Madrid seismic zone, central United States, *Geology*, v. 23, n. 3, p. 253-256.

Youd, T.L., et al., "Liquefaction Resistance of Soils: Summary Report from the 1996 NCEER and 1998 NCEER/NSF Workshops on Evaluation of Liquefaction Resistance of Soils," *Journal of Geotechnical and Geoenvironmental Engineering*, 127(10):817-833, 2001.

# Appendix A

## Evaluation of Scenario Earthquakes Using Liquefaction Potential Analysis

Appendix A

**Site Lee 1**
Water table at 1.5 m depth

**a. M 5.5 @ 5 km**

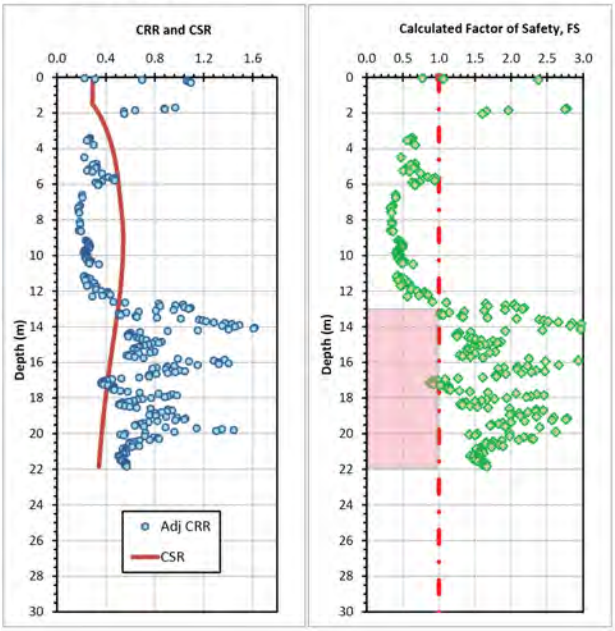


**b. M 5.5 @ 10 km**

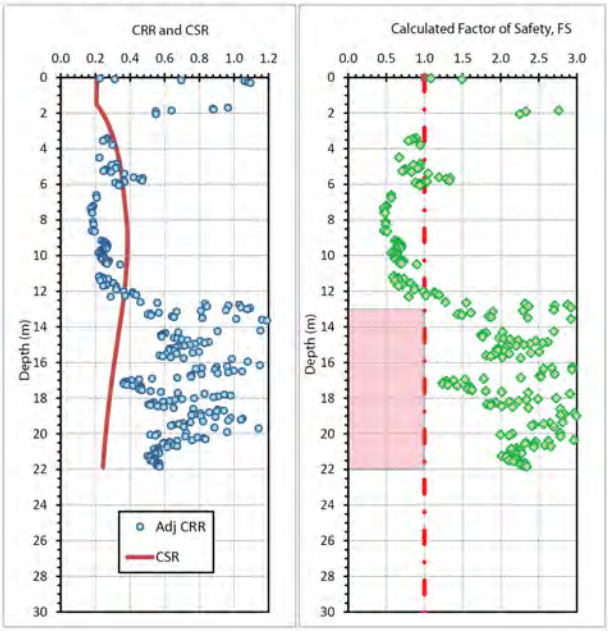


**c. M 6.0 @ 5 km**

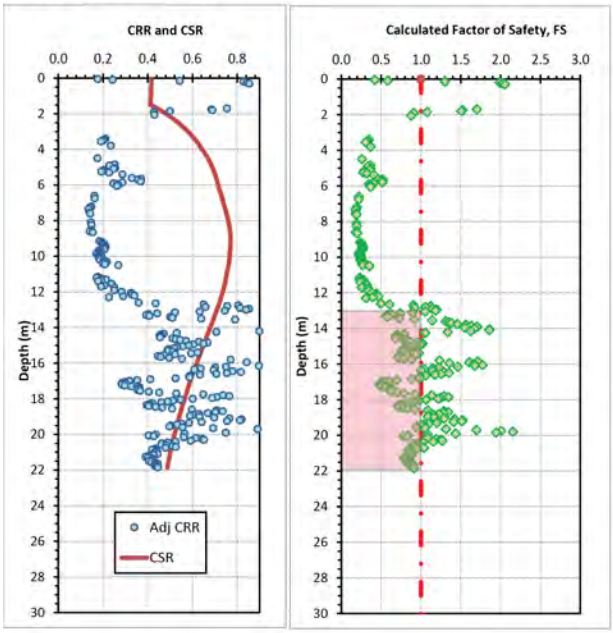


**d. M 6.0 @ 10 km**

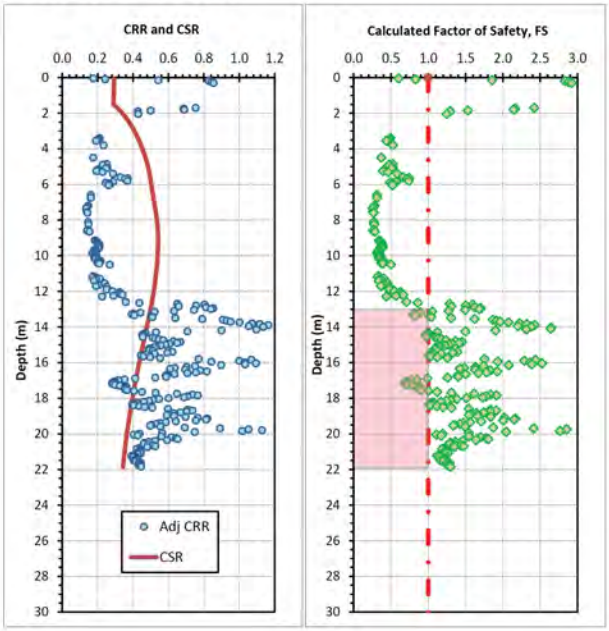

Appendix A

**Site Lee 1**
Water table at 1.5 m depth

**e. M 6.5 @ 5 km**

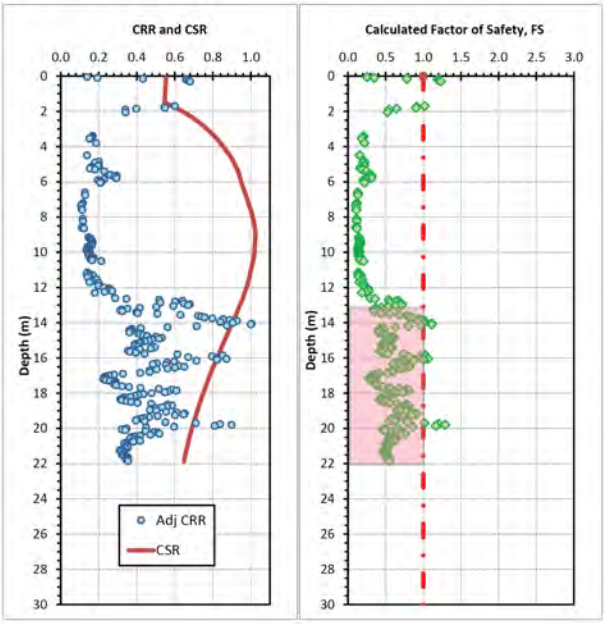


**f. M 6.5 @ 10 km**

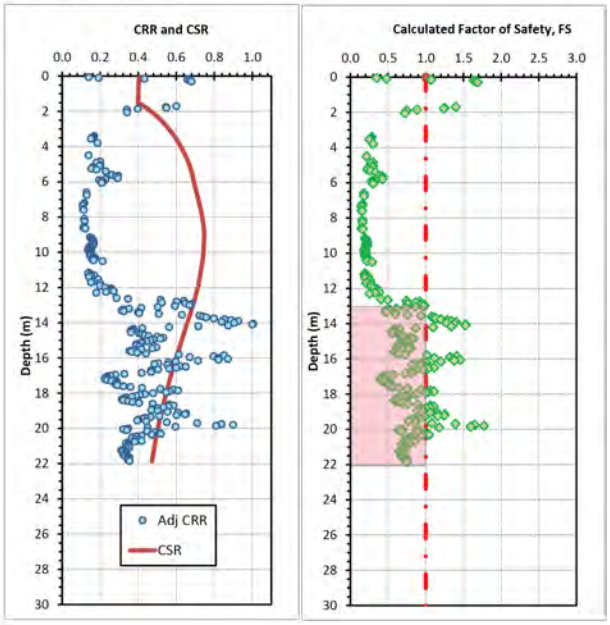

Appendix A

**Site Lee 1**
Water table at 5 m depth

**a. M 5.5 @ 5 km**

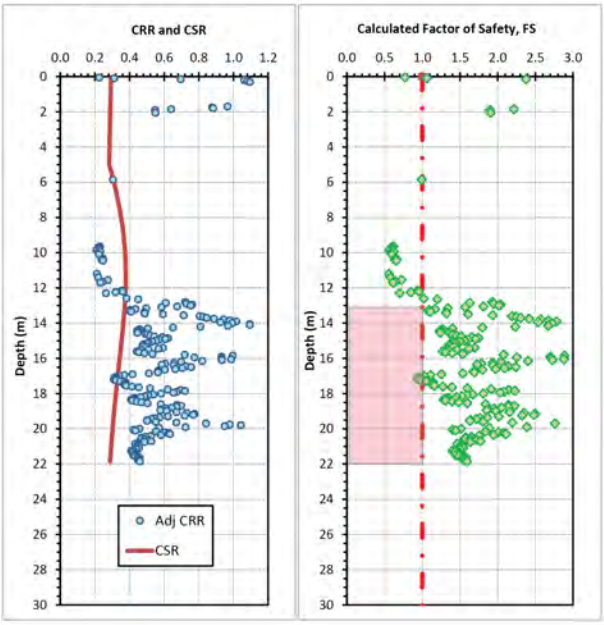


**b. M 5.5 @ 10 km**

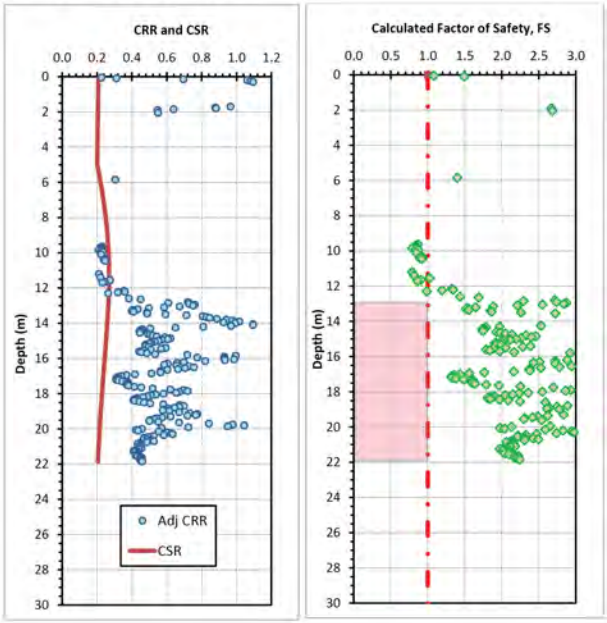


**c. M 6.0 @ 5 km**

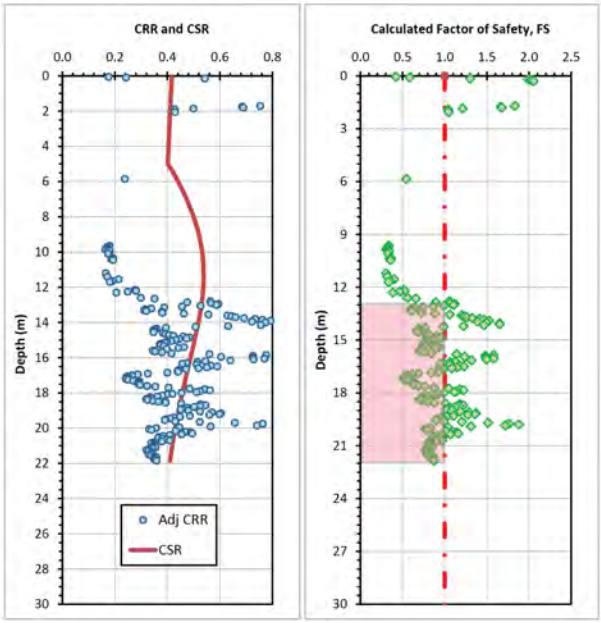


**d. M 6.0 @ 10 km**

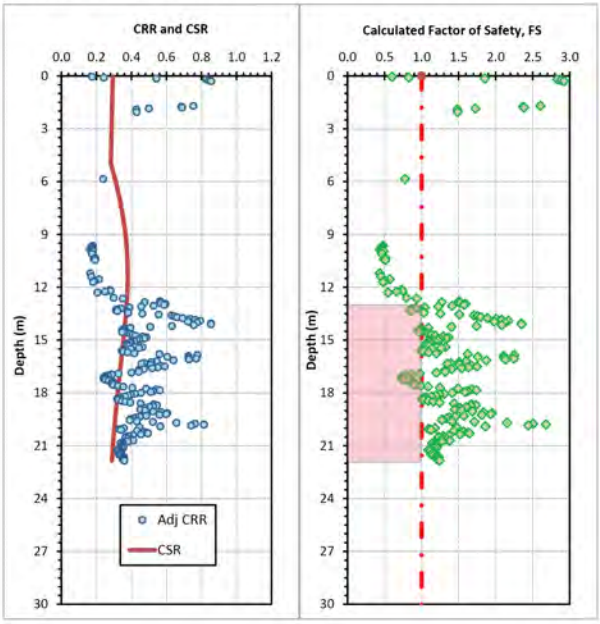

Appendix A

**Site Lee 1**
Water table at 5 m depth

**e. M 6.5 @ 5 km**

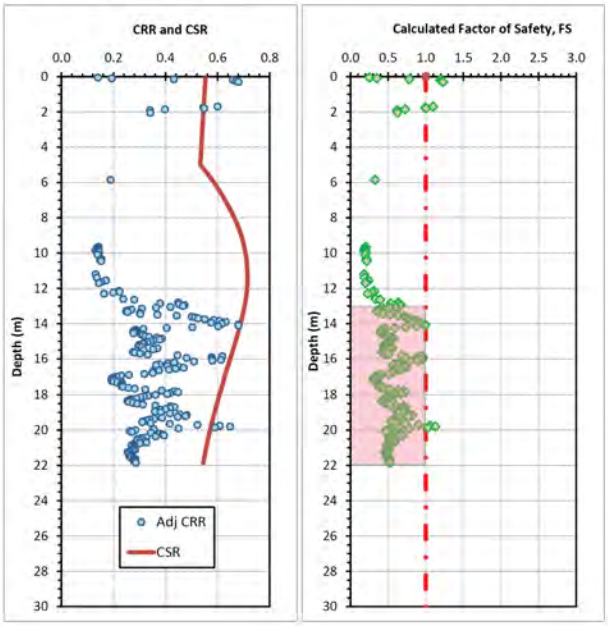


**f. M 6.5 @ 10 km**

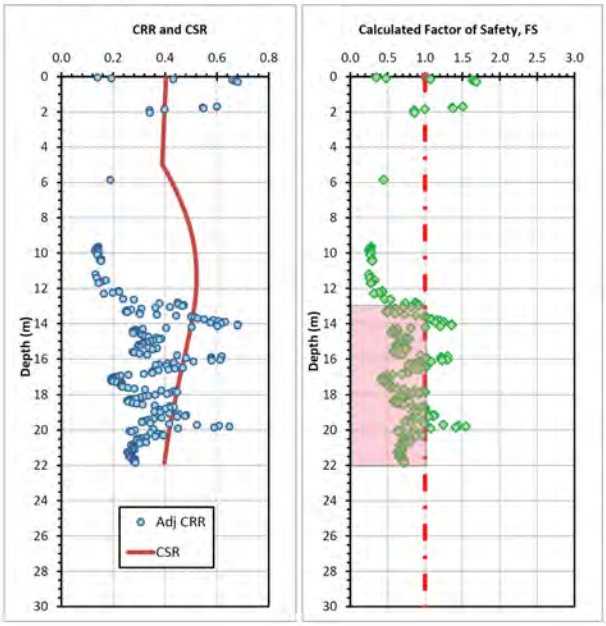

**Site Lee 3**
Water table at 1.5 m depth

**a. M 5.5 @ 5 km**

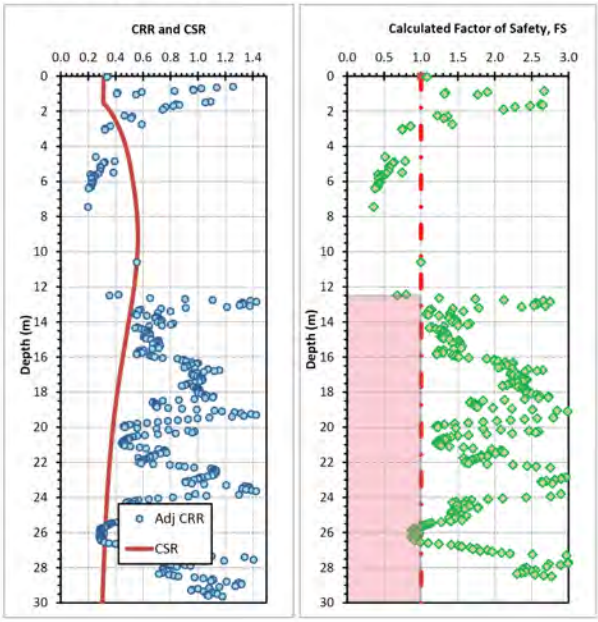


**b. M 5.5 @ 10 km**

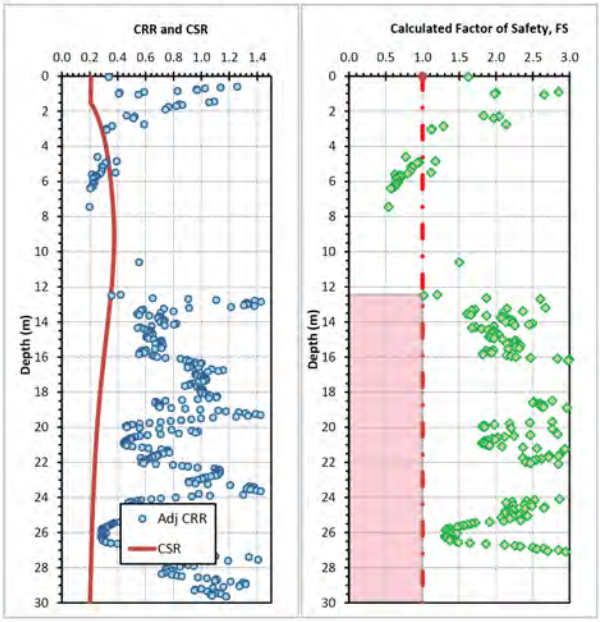


**c. M 6.0 @ 5 km**

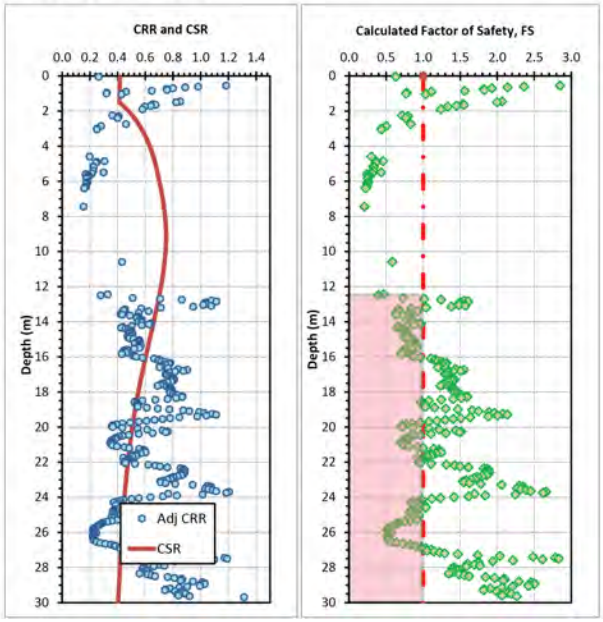


**d. M 6.0 @ 10 km**

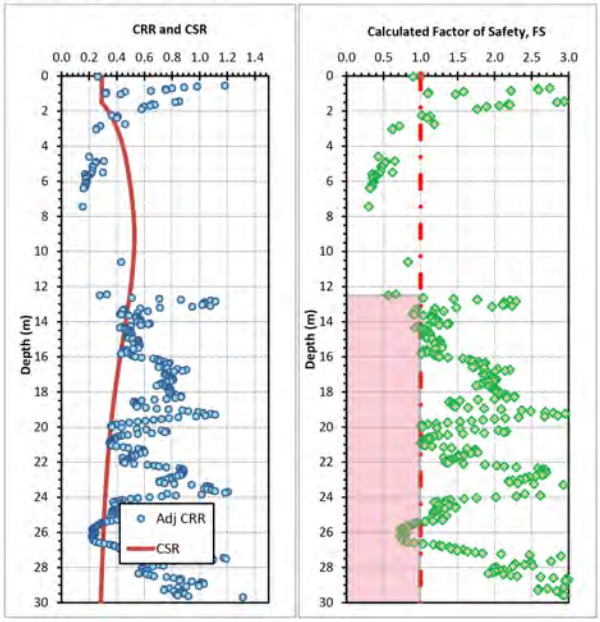

**Site Lee 3**
Water table at 1.5 m depth

**e. M 6.5 @ 5 km**

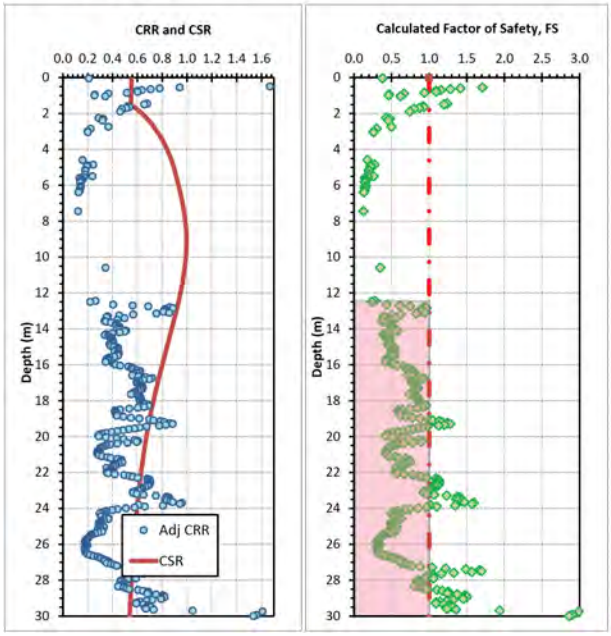


**f. M 6.5 @ 10 km**

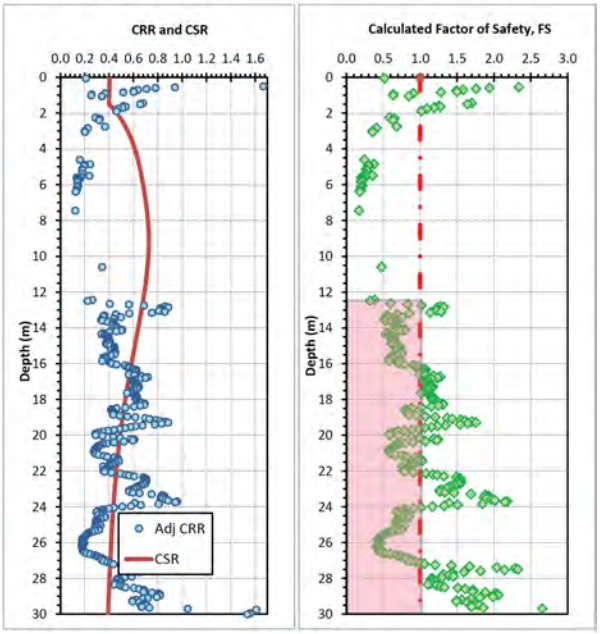

**Site Lee 3**
Water table at 5 m depth

**a. M 5.5 @ 5 km**

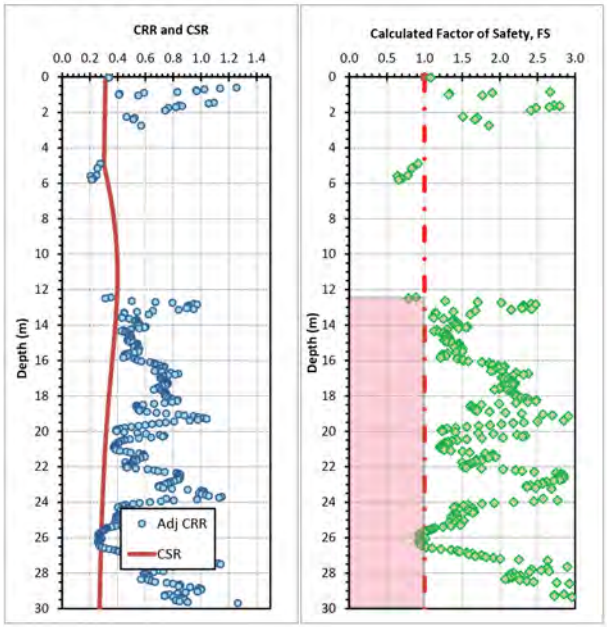


**b. M 5.5 @ 10 km**

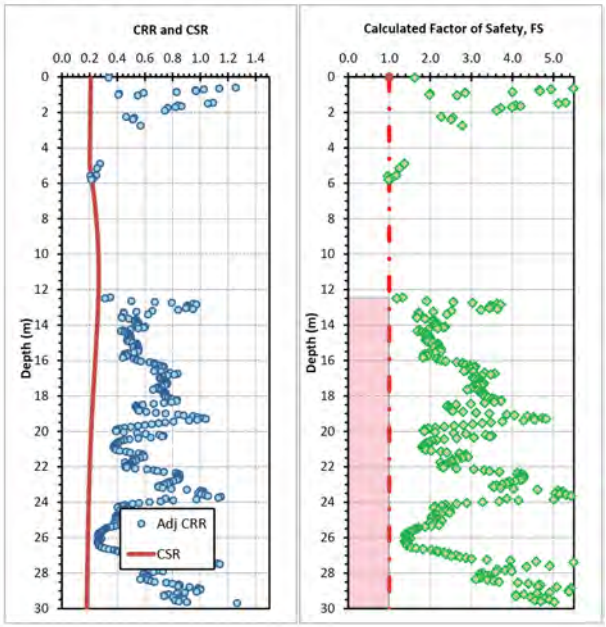


**c. M 6.0 @ 5 km**

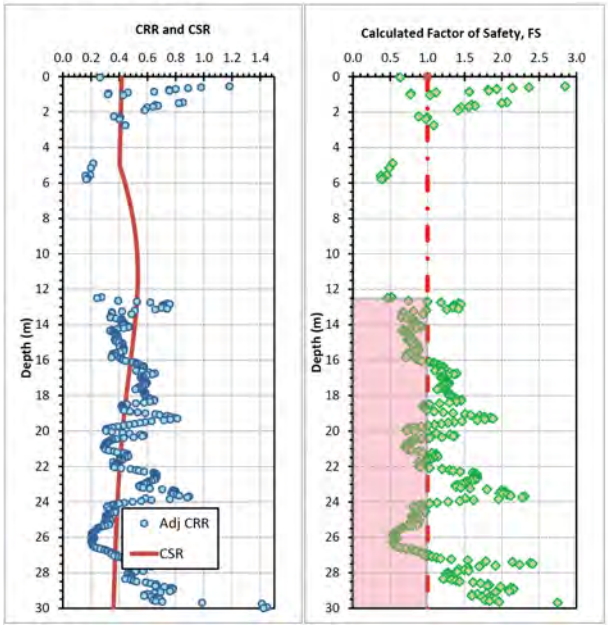


**d. M 6.0 @ 10 km**

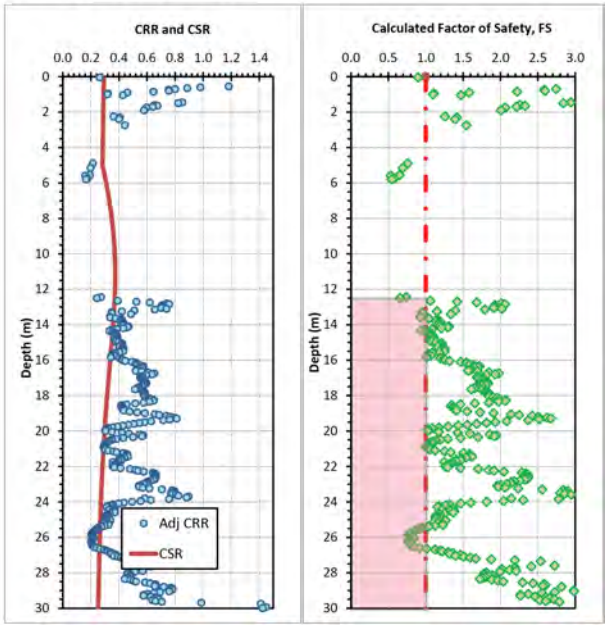

**Site Lee 3**
Water table at 5 m depth

**e. M 6.5 @ 5 km**

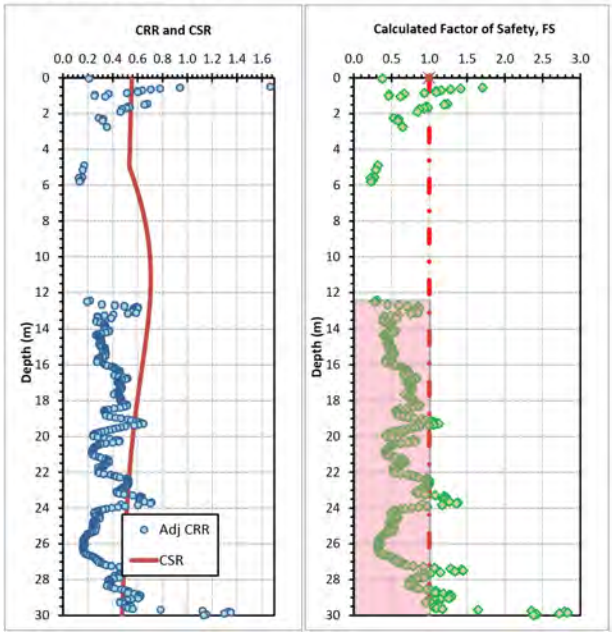

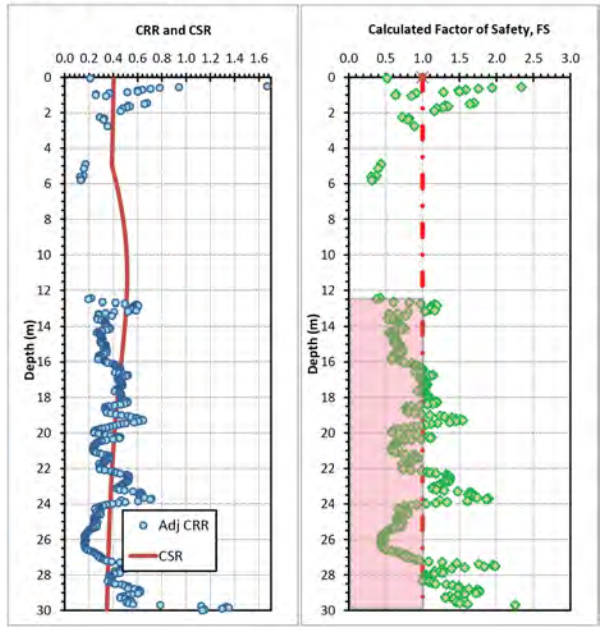
**f. M 6.5 @ 10 km**